The MONSTAR telescope:
Material Budget measurement

Antonín Lindner[1]

Supervisors:
Simon Florian Koch[2] and Brian Moser[1]

[1]CERN, Switzerland
[2]University of Oxford, United Kingdom

1 Introduction

The radiation length X_0 is an empirical quantity describing material budget effects of any object to the high-energy charged particles passing through. These effects are causing the particle to lose energy and scatter which is very undesired when measuring default particle properties. This is especially notable in the case of interaction vertex localization. The common way to measure the vertex is to use at least two silicon detectors with position resolution, where the particle is traversing both of them and is scattered by the first detector, adding an uncertainty on the position of the original interaction vertex. The radiation length X_0 is an important detector parameter desired to be minimised to reduce vertex position uncertainties and careful measurement is required to ensure the accuracy of simulations.

1.1 Radiation length

The radiation length X_0 is a material property representing the distance after which a high-energy particle lost enough energy by electromagnetic interactions with the material to reduce its energy by a factor 1/e. The radiation length can be measured using beam telescopes that measure the scattering angle distribution θ at the device under test (DUT).

The core of the angle distribution can be described by a Gaussian centered at zero with a standard deviation Θ which is related to X_0 through Highland's formula [1]:

$$\Theta = \frac{13.6 \text{ MeV}}{\beta c p} Z \sqrt{x/X_0}(1 + 0.038 \ln(x/X_0)) \tag{1}$$

where βc, p, Z are velocity, momentum and charge number of the scattering particle respectively. The x defines the thickness of the DUT. For larger angles, the scattering at the nucleus is contributing to the distribution as a Rutherford tail that follows a $1/\sin^4\theta$ distribution. The work inverts equation 1 to calculate the material budget x/X_0 from the measured distribution θ.

2 Experiment description

For the x/X_0 measurement the positron beam from the T9 beamline of the Proton Synchrotron located at CERN was used. A beam energy of around 1 GeV was chosen to ensure resolvable angles from multiple scattering and to maintain the relativistic properties of the positrons. The angle resolution is defined by the telescope geometry and the spatial resolution (pixel size) of the pixel sensors used in the telescope. Increasing the size of the telescope leads to larger deviations at the telescope plane but also adds volume of air that the positrons need to pass, resulting in undersired residual scattering that can substantially contribute to the systematic uncertainty of the x/X_0 determination.

2.1 The MONSTAR telescope

The Multiple Or Negligible Scattering Telescope, As Required (MONSTAR), shown in figure 1, was operated with four telescope planes, and either a DUT, or an inactive subject such as the air within the telescope. The DUT is symmetrically surrounded by upstream and downstream branches, each contains two MALTA chip pixel sensors - the 300 µm thick plane which is more distant from the DUT and the second 50 µm thick plane closer to the DUT [2]. This measurement was performed with an ITkPix v1.1 quad module designed for the ATLAS upgrade as DUT [3]. The DAQ part of the telescope utilizez each MALTA plane with an FPGA module controlled and synchronized by another FPGA module that functions as the trigger logic unit (TLU). The TLU is sending the trigger based on a coincidence of the outermost MALTA planes as these proved to be reliable and showed a low noise level. All of the FPGAs are equipped with an ethernet port to communicate with the DAQ PC via a local ethernet network. The ITkPix is readout via electrical cables and the signal is converted into an optical signal using a dedicated transciever board. A separate FELIX-based architecture is used to read out and send commands to the ITkPix module. The DAQ PC functions as the the master that controls all the peripherals. The event synchronization between the MALTA planes and the ITKPix module is done based on a simple consecutive counting of trigger signals.

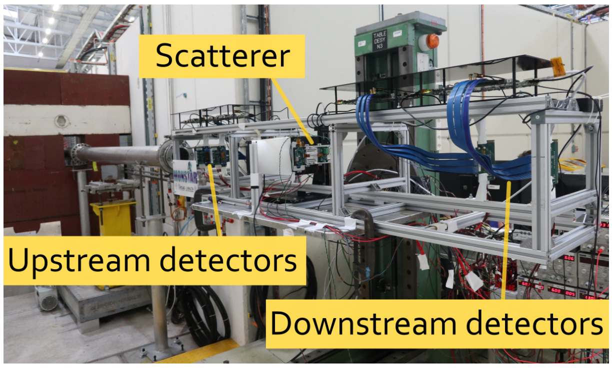

Figure 1: The Monstar telescope at T9 test beam area.

2.2 Data taking

The data taking was divided into three campaigns. In the first campaign the MALTA 50 µm plane was moved as far as possible from the DUT right next to the outermost MALTA 300 µm plane in both the upstream and downstream branch and a 700 MeV positron beam was used. In the second campaign the MALTA 50 µm plane was moved as close as possible to the DUT and a 1.2 GeV positron beam was used. The reason for these two configuration was to obtain comparable measurements with and without hits taken in the DUT in campaign two as the upstream and downstream tracks can be well reconstructed without DUT. This comparison can shed light on whether the material budget measurement can be done without positional information provided from the DUT, and as such the technique could be applied to an inactive subject such as a beam pipe or cooling infrastructure. The third campaign encompasses a range of exploratory configurations, including energy scans, reversing the orientation of the DUT along the x-axis, substituting a MALTA 50 µm plane as DUT, and measuring inactive subjects including the air within the telescope, and an ITkPix flex PCB without sensor. The telescope and beam configuration matches the second campaign.

As the area of the ITkPix sensor (40.2×38.6 mm) is larger than the area of MALTA planes (18.6×18.6 mm) it was required to use a x-y linear stage to move with the ITkPix in order to cover the entire area. In campaign 1 the ITkPix sensor surface was scanned in a 3×3 grid, whereas in campaign 2, a 4×4 grid was used. Due to the low positron rate and limited beam time the aim was set to obtain 2 million hits per cm^2, for which we expected to be able to obtain a spatial resolution of 0.5mm for our material map with a statistical uncertainty of 10 % or better. As the DUT was moving during the experiment, it was necessary to have different alignment across the positions in the first and second campaign. For this reason, before and after every positron beam data taking for each position, the data for the alignment was taken with a 15 GeV mixed hadron beam.

3 Analysis

To obtain the desired angle distribution for the x/X_0 map measurement, tracks must be reconstructed whilst allowing for a kink with the DUT, which relies on reconstructed clusters from hits in each plane, and a stable alignment of the telescope. The process of alignment and tracking has been performed with PyCorry [4] that adopts the Corryvreckan framework [5] and uses it for all the steps in analysis chain. The resulting angle distributions are fit using Parmesan-Fitter, which is adapted from the Parmesan framework [6].

3.1 Alignment

The final alignment used for the tracking is obtained in three steps. The first step consists in masking noisy pixels (i.e. the pixels with artificially high event counts), caused by defects in the sensor, or misconfiguration or misbehaviour of the analog frontend connected to this pixel. The **masking** is done using a local density method, adopted from the Proteus framework [7], where for the the tested pixel that holds $N_{x,y}$ events at position x, y, the average number of hits $\bar{N}_{x,y}$ and standard deviation $\sigma(N_{x,y})$ is being calculated from pixels with positions x', y' within the defined radius $R \geq \sqrt{(x-x')^2 + (y-y')^2}$ around the tested pixel. The pixel is being masked when exceeding a certain multiple N_σ of $\sigma(N_{x,y})$ over the $\overline{N}_{x,y}$, i.e. $N_{x,y} > \overline{N}_{x,y} + N_\sigma \sigma(N_{x,y})$.

Following step is the **prealignment** that computes the correlation matrices of the x_i and y_j coordinates between planes i and j (i. e. x_i vs x_j, x_i vs y_j and y_i vs y_j). The prealignment is then evaluated from the mean values of the correlation histograms that are being centered to zero. For multiple pixel planes, one needs to choosen a reference plane, against which the others are referenced (e.g. $i = 0$ and $j \in \{1, 2, 3, 4\}$ for the current telescope setup). The alignment itself is finalized by the Millepede algorithm [8], that uses a linear model least squares fit of the tracks for minimising the residuals. Figure 2 shows an example of the reduced χ^2 distribution of the linear track fitting on 15 GeV data after the alignment procedure.

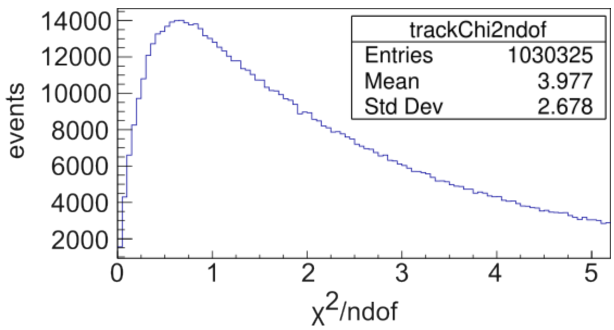

Figure 2: The reduced χ^2 distribution from a straight-line fit on 15 GeV data after alignment.

3.2 Tracking

As the analysis requires the measurement of kink angles caused by multiple scattering within the DUT, the particle track is represented by upstream and downstream tracks corresponding to linear tracks reconstructed from hits in the upstream and downstream detectors (see figure 3) respectively, where both can also include the DUT event cluster position into reconstruction. From such tracks the kink angle can be easily obtained.

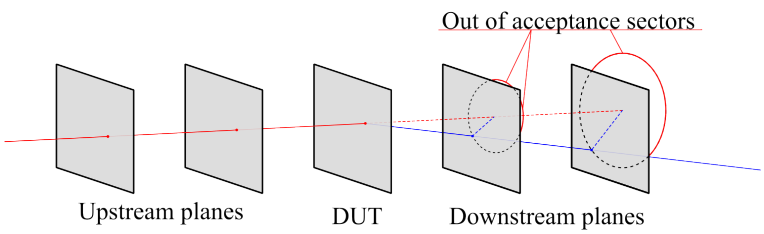

Figure 3: Upstream and downstream tracks with blind sectors.

3.3 Angle distributions

When assuming possible upstream tracks and their kink angles, some of the angles can have different acceptances resulting from geometrical constrains of pixel the planes. For this reason it is necessary to do an acceptance correction. Let upstream and downstream tracks, with angle θ between them, define a cone with its top at the point where upstream track crossed the DUT plane and the cone's shell is opening along the extrapolated upstream track that forms the cone's axis. The downstream track is moved such that it crosses the upstream track at the DUT plane and is included in the cone shell, so the cones opening angle is equal to θ. Such a cone than intersects the downstream planes and forms either full or partial ellipses. Let β_i represent the subtended angle of all arcs outside of the acceptance for the downstream plane i. Each event is then weighted by a value of $2\pi/(1 - \sum \beta_i)$ when filling the histogram. See figure 3 for an illustration of the correction.

In the analysis, three angles θ_g, θ_x and θ_y are extracted, corresponding to the global angle and the angle between the projected tracks to the x-y and the y-z planes respectively. When building a θ_g histogram, the acceptance of every bin is biased by corresponding area in the downstream planes (θ_x and θ_y are invariant). However, this area is roughly proportional to $\zeta = \left|\theta_b^2 - \theta_t^2\right|$ where θ_b and θ_t are the bins lower and upper edges respectively. In that case $1/\zeta$ is used as a weight when filling the histogram.

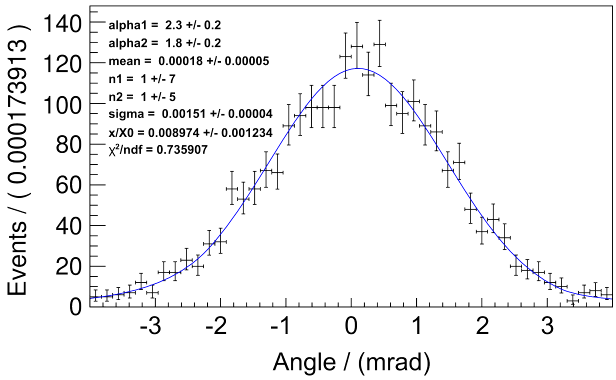

Figure 4: Example of a fit to the θ_x distribution.

3.4 Angle distribution fit and material budget map

Two dimensional histograms are built parameterising the position of tracks on the DUT plane. For this purpose, the DUT plane is separated into rectangle sectors with their size chosen such that a relative statistical uncertainty of 10% is expected. The standard deviation of the Gaussian core Θ from Highland's formula (equation 1) is extracted from a fit of the angle distribution using a Single or Double Sided Crystal Ball function (see figure 4), and afterwards x/X_0 is calculated using the inverse of Highland's formula.

4 Results

Following the described analysis methodology, the x/X_0 map was evaluated for campaign one and two (figure 5). However, the x/X_0 maps involve scattering on air and parts that are not part of ITkPix chip. These are the aluminium window frame machined into the chip holder and the feet from the 3D printed clamp - both highlighted on figure 5. The material budget of these features was subtracted from the map, based on a precise measurement of the material dimensions and weight, and the expected X_0 values for the respective materials. Only the air subtraction was based on the measurement with MALTA 50 µm plane as DUT. Since MALTA is a monolithic detector the material budget is well defined and evenly distributed over the chip area. The material budget is estimated to $(x/X_0)_{\mathrm{MALTA\ 50um}} = 0.5336$ % and the subtraction from its measurement gives the material budget contribution of air $(x/X_0)_{\mathrm{air}} = 0.4231$ %. However, the air subtraction is applicable only for campaign 2 that had same geometry as campaign 3. The aluminium holder window and dimensions were measured and also subtracted from both x/X_0 maps. The thickness of the window in the telescopes region of sight is (450.0 ± 3.9) µm which gives an expected material budget of the window $(x/X_0)_{\mathrm{window}} = 0.5058$ %. The last contribution that was subtracted was from the 3D printed clamp legs. Their material budget was estimated from a measurement of the mass and the volume of all three legs separately.

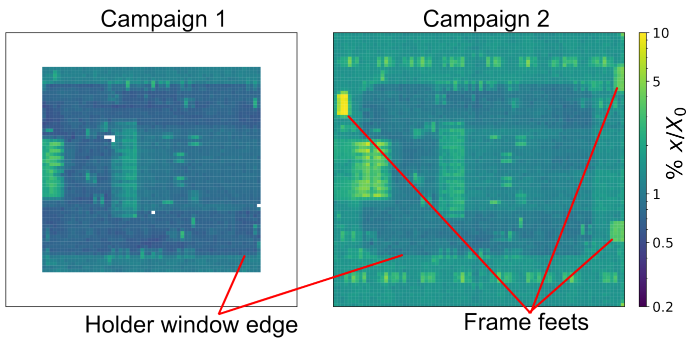

Figure 5: Evaluated x/X_0 maps for campaign 1 and 2 without removal of contributions from air and the module holder.

Both campaigns 1 and 2 results in 3 maps - $(x/X_0)_x$, $(x/X_0)_y$ and $(x/X_0)_g$ corresponding to measured angles θ_g, θ_x and θ_y respectively. And since $(x/X_0)_x$ and $(x/X_0)_y$ are independent, they are used to produce a combined material budget map

$$(x/X_0)_{\mathrm{combined}} = \left[\frac{(x/X_0)_x}{\sigma_x^2} + \frac{(x/X_0)_y}{\sigma_y^2}\right] / (\sigma_x^2 + \sigma_y^2) \ ,$$

where σ_x and σ_y are the uncertainties of $(x/X_0)_x$ and $(x/X_0)_y$ respectively. The uncertainty of $(x/X_0)_{\mathrm{combined}}$ is evaluated as $\sigma_{\mathrm{combined}} = \left[\frac{1}{\sigma_x^2} + \frac{1}{\sigma_y^2}\right]^{-1}$. The material budget map with from campaign 2 including all the above mentioned subtractions is shown in figure 6a.

4.1 Material budget estimation

To compare the measurement results, the material budget estimation was done based on the manufacturer drawing of the chip including the PCB flex board with its internal copper layers and surface masks, all SMD components and connectors mounted to the board, and the sensor layers. All these features were extracted or redrawn from manufacturer drawings and aligned a using vector graphics editor. Afterwards, the raster images were exported with pixels matching the real ITkPix sensor pixels, resulting in 2D maps of values $\in \langle 0, 1 \rangle$, where for the shape edges within the pixel the ratio of covered pixel area was used. For every layer, x/X_0 was estimated based on its thickness and X_0 values taken from Particle Data Group tables of materials atomic and nuclear properties [9]. However, some parts have a material composition which is not fully known so the ratio of materials was estimated intuitively. Estimated x/X_0 values were then used to scale the corresponding layer maps that were added to form the final material budget estimation [10]. This estimation is in figure 6b. Additionally, the subtraction from the measurement is shown in figure 6c (using a Gaussian kernel for filtering both material budget maps before subtraction).

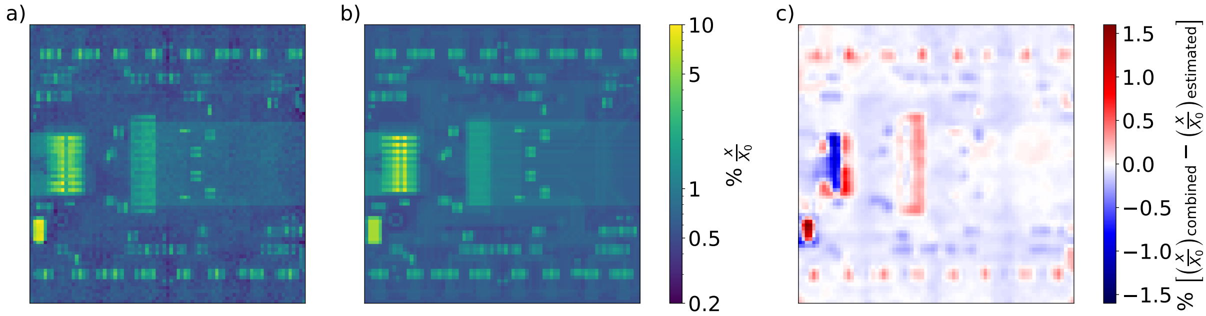

Figure 6: The material budget map of a) the measurement resulting from campaign 2, b) estimation and c) measurement and estimation filtered by Gaussian kernel with $\sigma = 1$ px and subtracted.

The plots in figure 6 give a good idea about the quality of measured material budget map. The structure of components match between the measurement and the estimation. In the subtraction plot, there are negative fluctuations (i.e. underestimation of material budget against the measurement) in regions where components are not present. However, at the component positions, both positive and negative values can be seen indicating the difference between estimation and measurement and demonstrating the necessity for the measurement presented in this report.

References

[1] G. R. Lynch and O. I. Dahl. Approximations to multiple coulomb scattering. *Nuclear Instruments and Methods in Physics Research Section B: Beam Interactions with Materials and Atoms*, 58:6–10, 1991.

[2] M. van Rijnbach et al. Performance of the MALTA telescope. *The European Physical Journal C*, 83(7), jul 2023.

[3] L. Meng. Atlas itk pixel detector overview, 2021.

[4] A. Lindner and S. F. Koch. PyCorry, 2023. Available at `https://gitlab.cern.ch/monstar-testbeam/pycorry`.

[5] L. Huth D. Dannheim, K. Dort et al. Corryvreckan: a modular 4d track reconstruction and analysis software for test beam data. *Journal of Instrumentation*, 16(03):P03008, mar 2021.

[6] S. F. Koch. Proteus-compatible Analyser/Resynchroniser for Multiple Electron Scatters across N planes, 2021. Available at `https://gitlab.cern.ch/sfkoch/parmesan`.

[7] M. Kiehn et al. Proteus beam telescope reconstruction, March 2019.

[8] V. Blobel and C. Kleinwort. A new method for the high-precision alignment of track detectors, 2002.

[9] R. L. Workman and Others. Review of Particle Physics. *PTEP*, 2022:083C01, 2022.

[10] A. Lindner and S. F. Koch. ITkPix material budget estimate for MONSTART measurement comparison, 2023. Available at `https://gitlab.cern.ch/monstar-testbeam/material-budget-estimate`.

A Material budget maps

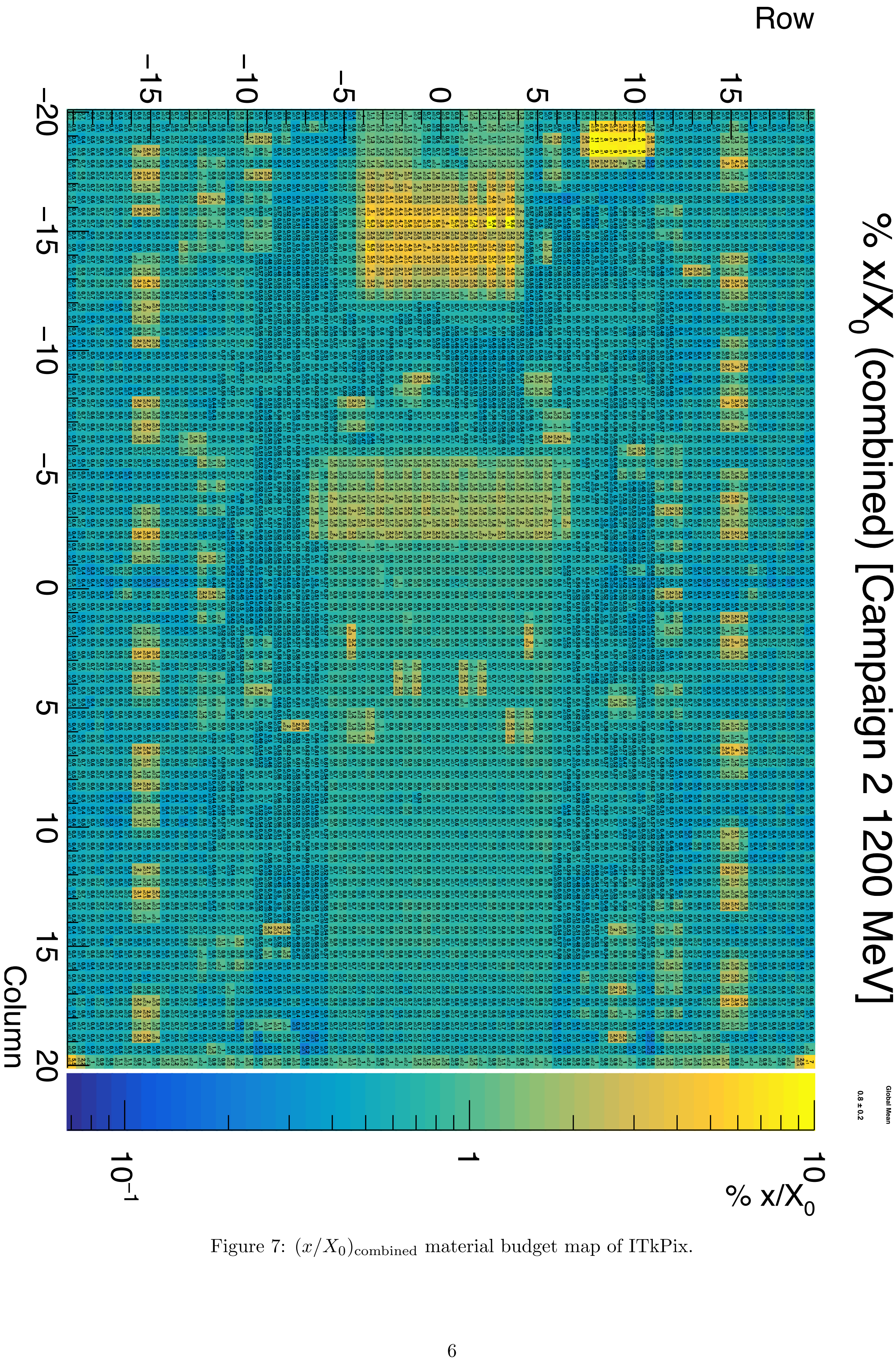

Figure 7: $(x/X_0)_{\text{combined}}$ material budget map of ITkPix.

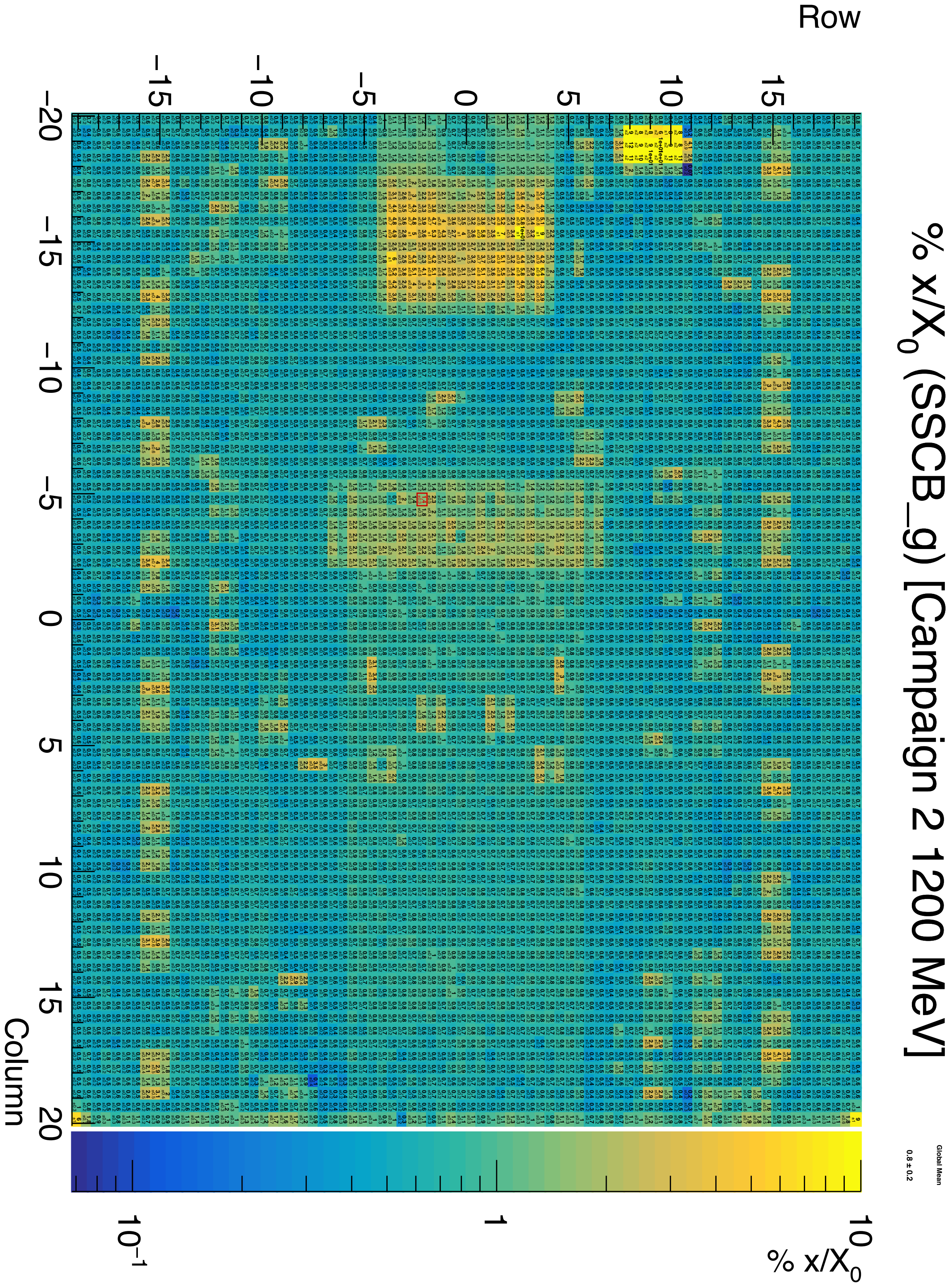

Figure 8: $(x/X_0)_{\mathrm{global}}$ material budget map of ITkPix.

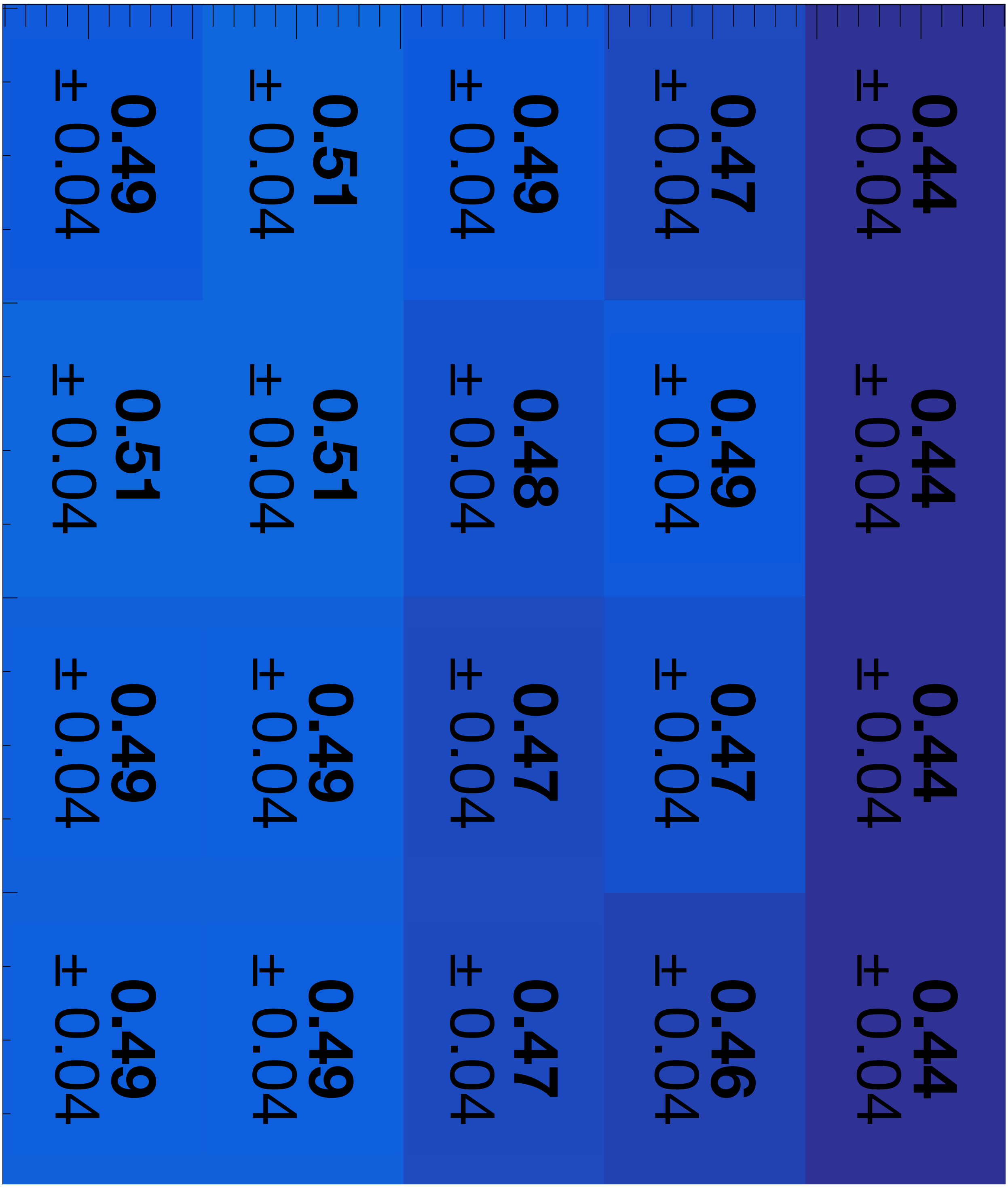

Figure 9: $(x/X_0)_{\mathrm{combined}}$ material budget map MALTA 50 µm.